

## EVIDENCE FOR TETHER-CUTTING RECONNECTION IN A QUADRUPOLE MAGNETIC CONFIGURATION IN THE APRIL 9, 2001, M7.9 FLARE

V. YURCHYSHYN

*Big Bear Solar Observatory, Big Bear City, CA 92314, U.S.A.*

M. KARLICKÝ

*Astronomical Institute of the Academy of Science of the Czech Republic, 25165 Ondřejov,  
Czech Republic*

Q. HU

*IGPP, University of California, Riverside, CA 92521, U.S.A.*

and

H. WANG

*Center for Solar Research of New Jersey Institute of Technology, Newark, NJ 07102, U.S.A.*

(Received 5 July 2005; accepted 17 February 2006)

**Abstract.** We studied the M7.9 flare on April 9, 2001 that occurred within a  $\delta$ -sunspot of active region NOAA 9415. We used a multi-wavelength data set, which includes *Yohkoh*, TRACE, SOHO, and ACE spacecraft observations, Potsdam and Ondřejov radio data and Big Bear Solar Observatory (BBSO) images in order to study the large-scale structure of this two-ribbon flare that was accompanied by a very fast coronal mass ejection (CME). We analyzed light curves of the flare emission as well as the structure of the radio emission and report the following: the timing of the event, *i.e.*, the fact that the initial brightenings, associated with the core magnetic field, occurred earlier than the remote brightening (RB), argue against the break-out model in the early phase of this event. We thus conclude that the M7.9 flare and the CME were triggered by a tether-cutting reconnection deep in the core field connecting the  $\delta$ -spot and this reconnection formed an unstable flux rope. Further evolution of the erupted flux rope could be described either by the “standard” flare model or a break-out type of the reconnection. The complex structure of flare emission in visible, X-ray, and radio spectral ranges point toward a scenario which involves multiple reconnection processes between extended closed magnetic structures.

### 1. Introduction

Solar flares and coronal mass ejections (CME) result from global changes in solar magnetic fields. Existing CME models predict that eruption begins when a magnetic structure (*e.g.*, a flux rope or a sheared arcade), becomes unstable, and rapidly expands into the corona. Such an expanding structure may further evolve catastrophically, when major magnetic reconnection and energy release take place, and be rapidly accelerated to speeds exceeding  $2000 \text{ km s}^{-1}$ . Besides the strong emission from the flare core, remote emission is also observed in  $H\alpha$ , EUV, and X ray

spectral ranges, and it is thought to be related to the large-scale structure of the flare (Wang, 2005). Other solar surface activity such as plasma flows (Wang *et al.*, 2001), appearance of trans-equatorial loops (Pevtsov, 2000; Harra, Matthews, and van Driel-Gesztelyi, 2003) and the large-scale dimming (Thompson *et al.*, 1998; Wang *et al.*, 2000) provide another important hint about the large-scale structure of solar flares and CMEs.

This study focuses on the large-scale structure of the April 9, 2001 eruptive flare, in particular on the temporal and spatial relationships between various sources of  $H\alpha$  emission and the related quadrupole magnetic configuration. Remote emission is often observed in  $H\alpha$  and/or EUV as a chain of RBs in different parts of a flaring active region and/or quiet sun areas. LaBonte (1976), and Tang and Moore (1982) reported that remote brightenings (RBs), observed in  $H\alpha$ , coincide in time with type III reverse slope (RS) radio bursts that are the descending part of U bursts and are generated by fast moving electrons channeled along closed magnetic loops. Those electrons first move upward from the acceleration site along one leg of a loop and then downward toward the photosphere in the opposite leg of the loop. The slow frequency drift of the reverse bursts speaks in favor of a long trajectory of the corresponding beams (Tarnstrom and Zehntner, 1975). When these fast electrons, associated with the reverse bursts, reach the chromosphere they may cause remote  $H\alpha$  emission. Note that RS bursts can also be generated by electron beams directly propagating downwards from the acceleration space.

Manoharan *et al.* (1996) considered a series of radio bursts and corresponding remote X-ray brightenings as a signature of a large-scale reconnection process between an expanding current carrying loop and large-scale overlying loops. Wang *et al.* (2002) studied the November 24, 2000 flare and found that there were two stationary ribbons near the leader spot and the third ribbon was moving away from the flare site. They proposed that the remote ribbon is due to interaction between the erupted flux rope of the flare core and the overlying arcade field.

Yurchyshyn *et al.* (2004) studied the July 23, 2002  $\gamma$ -ray flare and found that about 7 min after the onset of the flare several remote  $H\alpha$  brightenings and a 2218–2228 keV  $\gamma$ -ray source appeared in the active region. The light curves of the  $\gamma$ -ray source and the RBs were similar, though the  $\gamma$ -ray source peaked approximately 60 s after the peak of the RBs curve. The similarity of the time profiles and the 60 s lag is suggestive that those two emission sources are related to one common process that accelerated both electrons and ions (see Hurford *et al.*, 2003). This can possibly be due to reconnection between the erupted field and the large-scale magnetic field spanning the active region (for more discussion see Yurchyshyn *et al.*, 2004).

Here we analyze the M7.9 flare on April 9, 2001 that occurred in active region NOAA 9415 near the center of the solar disk. This active region was extremely productive and it launched numerous X-ray flares and CME (Tian, Liu, and Wang, 2002; Asai *et al.*, 2003; Sakurai and Hagino, 2003). Liu *et al.* (2005) reported changes in the penumbra area associated with the M7.9 flare. A preliminary analysis of the radio data from the flare was performed by Ceccato *et al.* (2002). We will use

a multi-wavelength data set from *Yohkoh*, TRACE, SOHO, and ACE spacecraft, Potsdam and Ondřejov radio telescopes and Big Bear Solar Observatory  $H\alpha$  images and longitudinal magnetograms in order to study the large-scale structure of the flare.

## 2. Observations

The April 9, 2001 M7.9 two-ribbon flare occurred in a  $\delta$ -type active region (Figures 1 and 2) and was associated with a very fast halo CME first observed in the SOHO/LASCO C2 field of view at 15:54 UT. The  $H\alpha$  flare emission started at 15:22 UT (Figure 3) as two bright patches in areas A2 and A3 (Figure 1) located within the  $\delta$ -spot. GOES 0.5–4 Å flux began to increase at 15:23 UT (shaded area in Figure 3), while the rise of *Yohkoh*/HXR emission was delayed by about 30 s (blue dashed line). At this time, in the first two  $H\alpha$  patches emission was on the rise and they reached their maximum intensity at 15:25 UT. The flare area began to expand and several additional  $H\alpha$  brightenings appeared at 15:24 UT (A4 and A5) and at 15:28 UT (A1). Eventually, A2 and A3 continuously evolved into fully developed flare ribbons. This fact implies that energy release started in the sheared core flux and then continued into the main phase. We also note that the diffuse facular area between A1, A2, and A3 did not brighten during this flare. At least no visible and notable increase in the brightness was observed. This area was associated with another flare on April 10. In Figure 2, we show a BBSO line-of-sight magnetogram taken 1 h after the flare onset and linear force-free lines (LFFF) calculated with the parameter  $\alpha = 0.01 \text{ arcsec}^{-1}$  ( $0.00725 \text{ Mm}^{-1}$ ). In this image, A2 and A3 are associated with the  $\delta$ -spot under consideration, which consisted of two opposite polarities umbrae within one common penumbra. According to the LFFF model, A1 was magnetically connected with the site of the flare (A2), as well as A5 was connected to A4 and A3, where footpoints of the post-flare loops were located. Note that the magnetic connectivity was not significantly affected when  $\alpha$  values in our simulations were changed from 0.008 to  $0.01 \text{ arcsec}^{-1}$ . The pre-flare *Yohkoh* and TRACE images (Figures 2 and 4) provide observational evidence for these magnetic connections.

In the pre-flare 15:09 UT *Yohkoh* image, we indicate the position of core fields that were located between the initial brightenings at A2 and A3. We argue that those field lines were strongly sheared because the emission ridge in the 15:09 UT *Yohkoh* image is oriented nearly parallel to the neutral line, which is different from the orientation of the simulated field lines in Figure 2, which were obtained with a rather small value of parameter  $\alpha$ . Also, the location of the initial  $H\alpha$  brightenings, A2 and A3, is displaced in the direction along the inversion line (A2 southward and A3 northward), which corresponds here to positive helicity (positive parameter  $\alpha$ ). These core fields connected the innermost parts of the two umbrae that comprised the  $\delta$ -configuration. We suggest that a tether-cutting type of reconnection in the

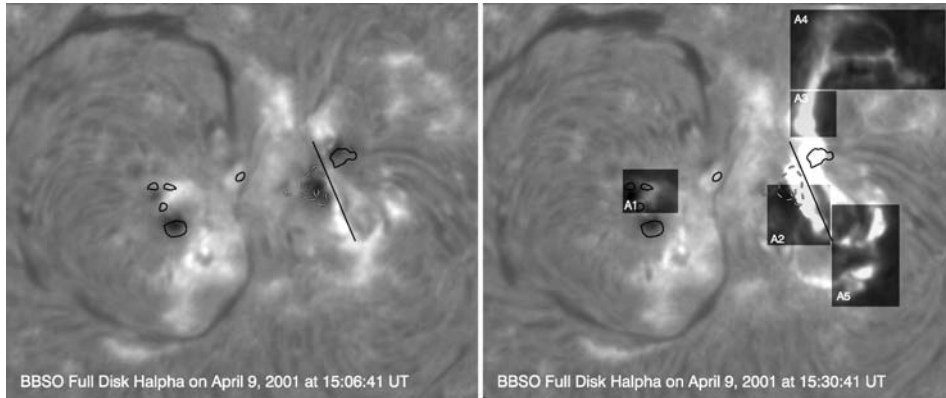


*Figure 1.* BBSO  $H\alpha$  images of active region NOAA 9415 before the M7.9 flare (*left*) and with the flare (*right*). Darkened boxes indicate the areas that were used to calculate the light curves. The black contours show the  $\pm 1000$  G level (*solid/dashed*) as measured from full disk MDI magnetograms and thus mark the position of the two umbrae within the  $\delta$ -spot. Note that the same contours are plotted over *Yohkoh* images in Figure 4. A segment of the *black line* marks the position of the neutral line within the  $\delta$ -configuration. North is to the top, west is to the right.

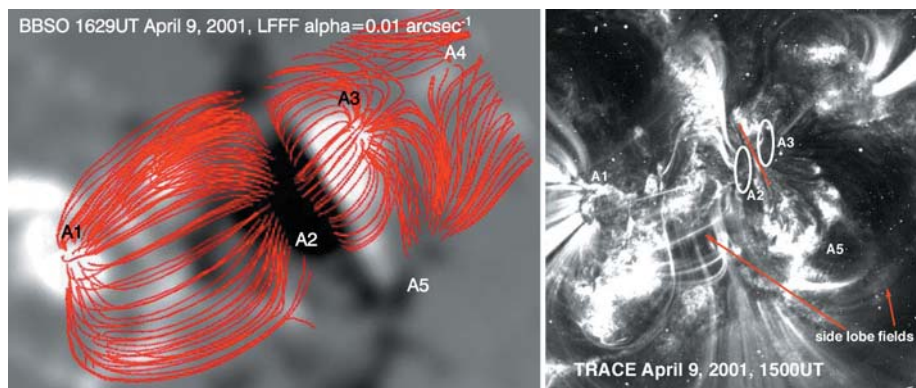


*Figure 2.* *Left:* BBSO  $223 \times 256$  arcsec longitudinal magnetogram of AR NOAA 9415 with overplotted linear force-free field lines. *White/black* represent positive/negative polarity. *Right:* A pre-flare TRACE  $171 \text{ \AA}$  image taken at 15:00 UT. A line segment between A2 and A3 marks the position of the neutral line. Two *white ellipses* mark the position of the two umbrae within the  $\delta$ -configuration. Side lobe fields are indicated by the *arrows*.

core field most probably formed a flux rope and triggered the eruption in this active region.

In the radio range, the flare started at 15:23:30 UT by a radio flux increase at 3 GHz and by weak pulsations in the 250–500 MHz frequency range (Figures 3, 5, and 6). On 3 GHz, the flare, as a whole, was characterized by four strong quasi-periodic main bursts that peaked at 15:26, 15:30, 15:37, and 15:45 UT (the first three are shown in Figure 3). In the metric range, these pulsations were followed

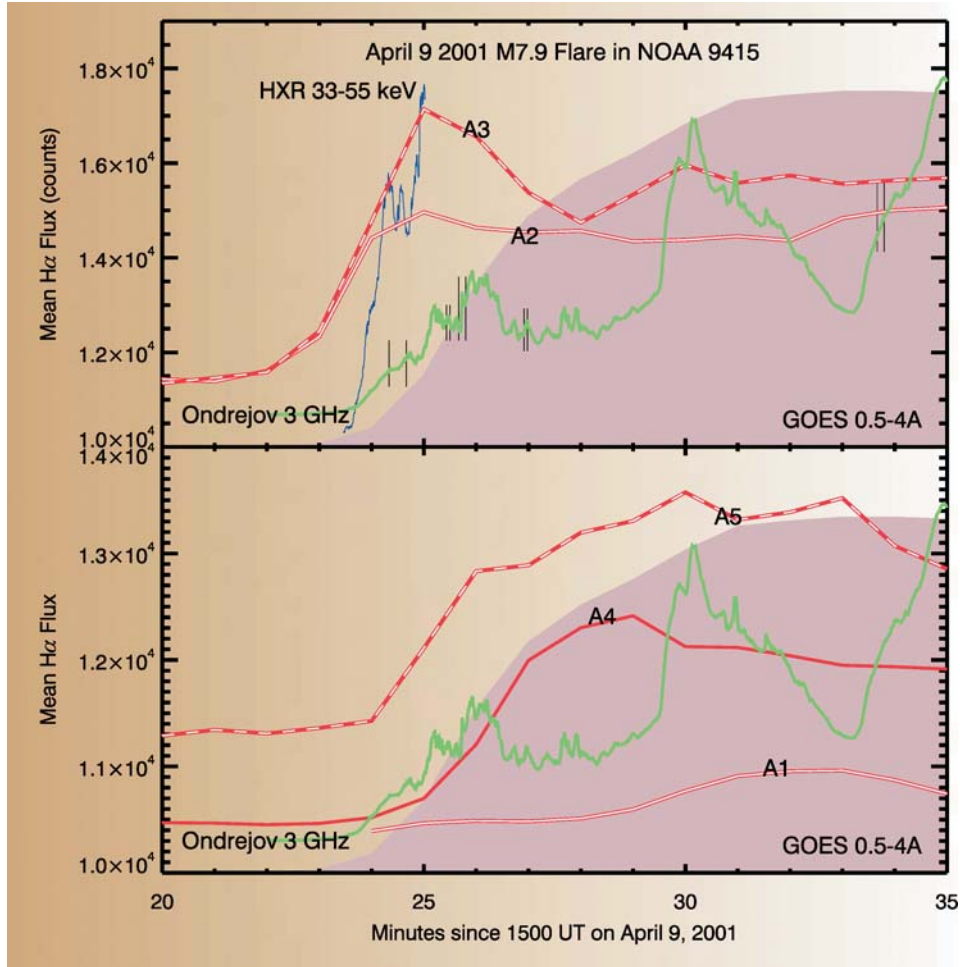


Figure 3. Light curves for the M7.9 flare. All  $H\alpha$  light curves are plotted with various red lines and are determined in areas A1 – A5, as shown in Figure 1. In both panels, the shaded area shows GOES 0.5 – 4Å X-ray flux and the blue line in the upper plot shows *Yohkoh*/HXR emission. The spiky green solid line is the radio flux at 3 GHz. The short segments of vertical lines indicate the periods when strong type III RS bursts were observed.

by a type II burst (flare shock) at 15:25 – 15:50 UT in the range of 40 – 300 MHz and by a type III bursts (electron beams propagating upwards in the solar corona) in the 40 – 400 MHz range at 15:27 – 15:40 UT (Figure 5). On higher frequencies, a long-lasting slowly drifting pulsation structure was observed between 15:25 and 15:50 UT. It started at about 1 GHz and drifted with the mean drift rate of  $\sim -1 \text{ MHz s}^{-1}$  towards lower frequencies. After reaching the frequency of 300 MHz at 15:50 UT, the drifting structure decayed. If we assume radiation on fundamental plasma frequency, we can thus obtain that this slow drifting structure at 800 MHz was located at height of about 18 000 km (15:27:30 UT), while at 15:47:30 UT it

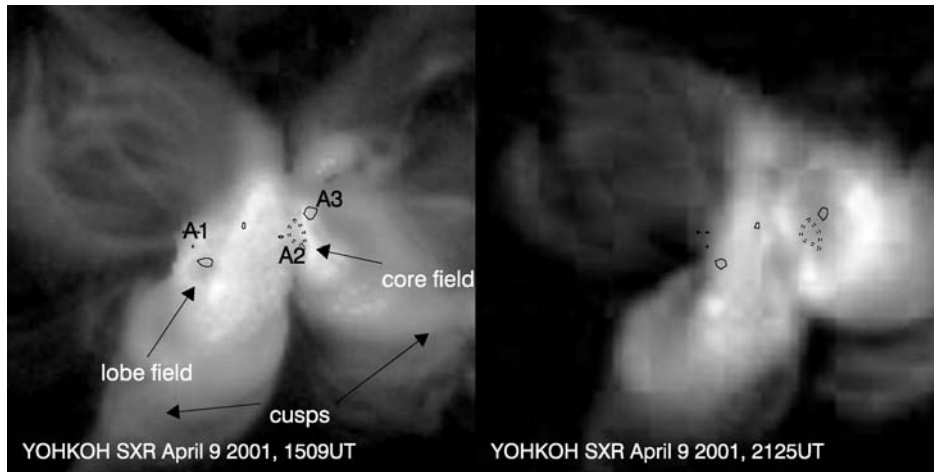
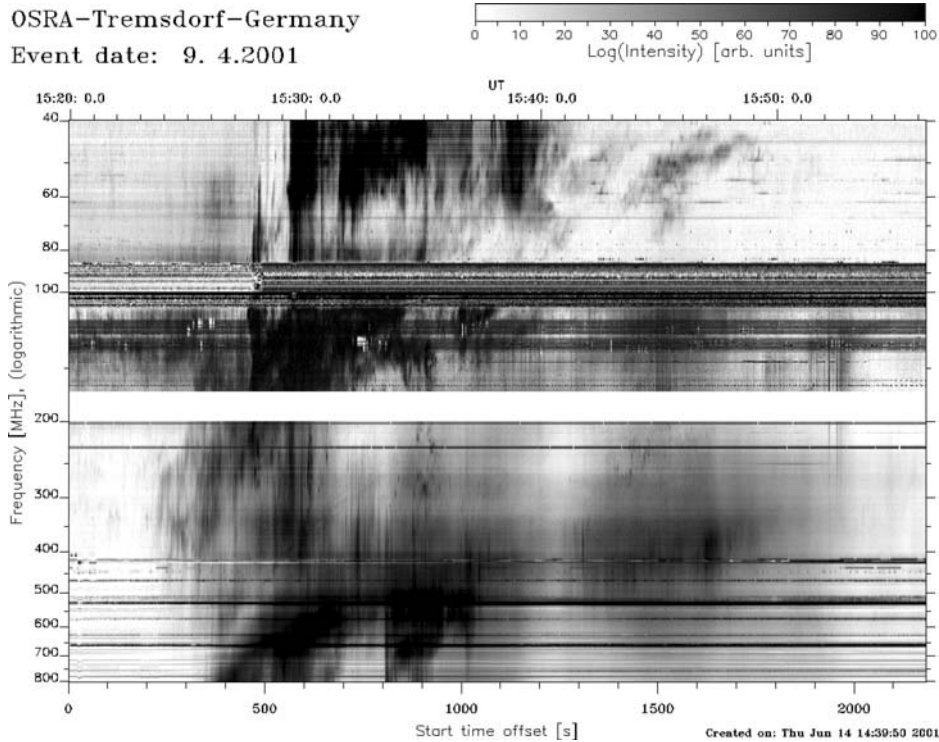


Figure 4. *Yohkoh* images of AR NOAA 9415. The arrows in the pre-flare 15:09 UT *Yohkoh* image (left) indicate the sheared core field and side lobe fields as well as the cusp-like structures. The black contours show the  $\pm 1000$  G level (solid/dashed) as measured from full disk MDI magnetograms and thus outline the position of the two umbrae that comprise the  $\delta$ -configuration. The images were scaled jointly so that the same level of gray corresponds to the same flux.

was seen at 400 MHz, which corresponds to height of 32 000 km (Aschwanden, 2002). The mean upward drift velocity thus estimated is about  $12 \text{ km s}^{-1}$ . For these estimations, we used a density model for type III emitting flux tubes presented in Figure 112 of Aschwanden (2002). This model is the most commonly used density model for estimations of height from dynamic radio spectra (assuming plasma emission processes), especially for high frequencies (see radio frequencies in this figure).

At high frequencies, this slowly drifting structure was associated with many slow and fast type III RS bursts that looked as a descending part of the type U burst, for example, at 15:25:26–15:25:30 UT in the 1.4–2.7 GHz range, and at 15:25:40–15:25:48 UT in the 1.0–2.0 GHz range (Figure 6; see Cecatto *et al.*, 2002, and Figure 111 in Aschwanden, 2002). In addition to those shown in the figure, a similar fast type III RS burst was also observed at 15:24:20–15:24:40 UT in the 1.6–2.8 GHz range. Examples of a slow RS burst with drift rate of  $+200$  to  $+600 \text{ MHz s}^{-1}$ , can be seen as a descending part of the U-burst (ellipse in Figure 6) and between 15:26:56 and 15:26:58 UT at 1600–2000 MHz (drift rate  $+200 \text{ MHz s}^{-1}$ ). A group of fast RS bursts (drift rates  $+980$  to  $+1720 \text{ MHz s}^{-1}$ ) were observed between 15:33:40 and 15:33:48 UT at 1700–2300 MHz (see also Cecatto *et al.*, 2002) and between 15:25:25.8 and 15:25:26.2 UT at 3500–4500 MHz (drift rate  $+2500 \text{ MHz s}^{-1}$ , Figure 6). Some fast drifting bursts were observed even in the range of 3.0–4.5 GHz. All those periods are indicated in Figure 3 by short vertical lines.

Due to high rate of radio bursts, it is difficult to recognize a clear type U burst. Only in one case at 15:25:14–15:25:16 UT in the 3.1–3.7 GHz range, we can distinguish a very weak type U burst (Figure 6). Nevertheless, it is highly probable



*Figure 5.* The composite radio spectrum in the range of 40.0–800.0 MHz observed during the April 9, 2001 flare by the Potsdam Tremsdorf OSRA instrument (courtesy of A. Klassen). In the range below 200 MHz, it shows the type II radio burst and group of type III bursts. At higher frequencies (>300 MHz) we can see slowly drifting structure after 15:25 UT.

that some reverse drift bursts are descending legs of type U bursts. Similarly, some type III like bursts in this case can be the ascending legs of U bursts.

At about 15:28 UT, at frequencies above 2 GHz, the gyro-synchrotron emission component started to be dominant. The gyro-synchrotron emission is generated mainly by electrons gyrating perpendicularly to the magnetic field and is proportional to the intensity of the magnetic field. The increase in the gyro-synchrotron emission starts nearly at the same time as the RB at A1 (Figures 1 and 3).

### 3. Discussion and Conclusions

The structure of the flare emission favors an idea that multiple large-scale magnetic structures, associated with a quadrupolar magnetic topology, interacted during the flare; however, many details remain hidden due to the complexity of the event and the limited resolution of the data.

From the fact that the  $H\alpha$  sources A2 and A3, which are the closest to the core field of all sources, brightened up clearly before the remote  $H\alpha$  brightenings, we

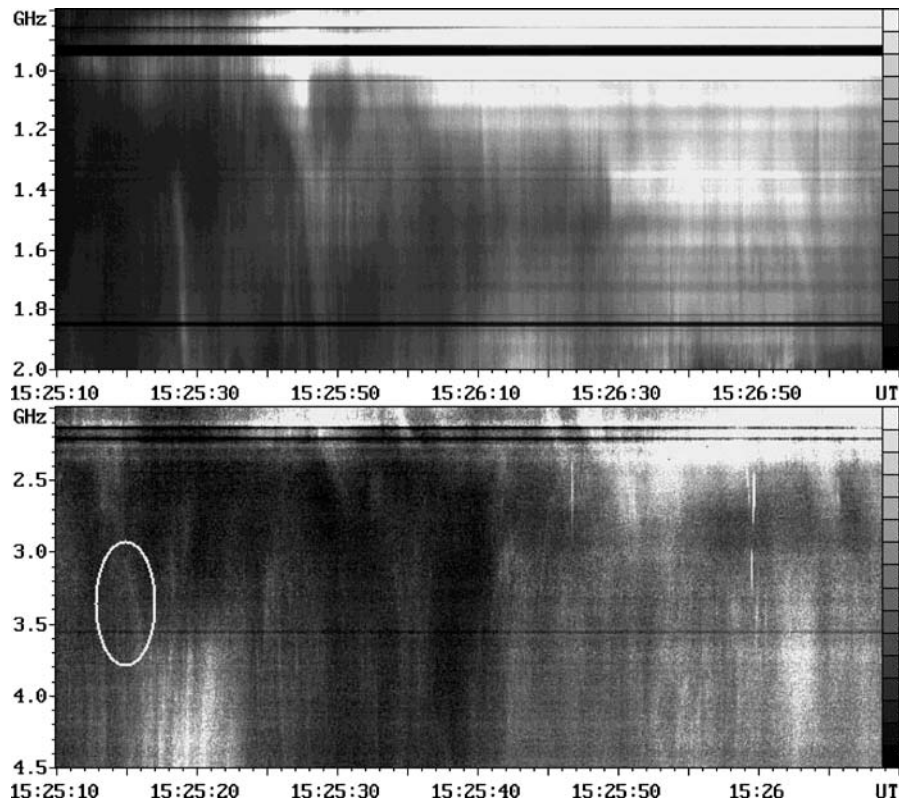
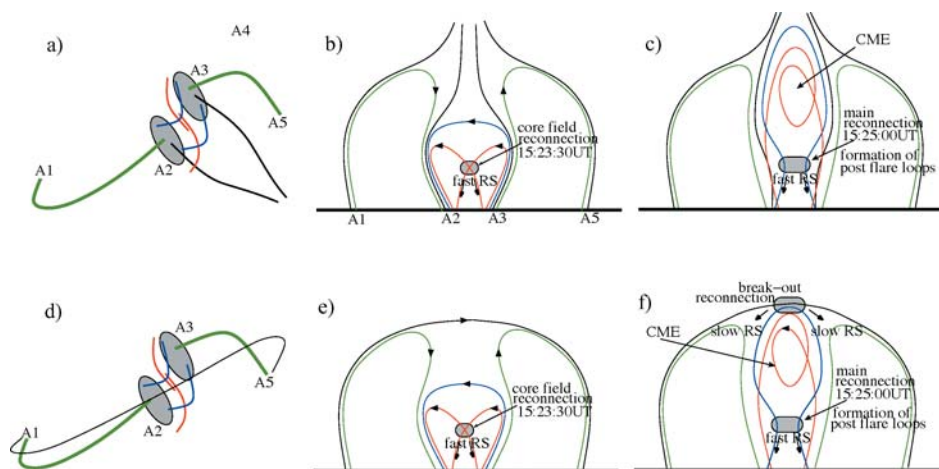


Figure 6. Radio spectra in the 0.8–2.0 GHz (*top*) and 2.0–4.5 GHz (*bottom*) range observed during the April 9, 2001 flare by Ondřejov radiospectrograph (emission is *white*). Spectra show groups of many type III reverse slope bursts (*e.g.*, between 15:25:40 and 15:25:48 UT in the 1.0–2.0 GHz range). Because of high rate of radio bursts, it is difficult to recognize a clear type U burst. Only in one case, a very weak type U burst was distinguished (indicated in the *lower panel* by the ellipse). It is probable, however, that some RS bursts are descending part of type U bursts and, similarly, some type III like bursts can be the ascending legs of U bursts.

conclude that the April 9, 2001 flare and the CME were triggered by the initial, tether-cutting type of reconnection (see Moore and LaBonte, 1980; Moore *et al.*, 2001) deep in the core field, which connected the innermost parts of the  $\delta$ -spot (Figure 7a and b, red lines). We propose that the sudden increase of the  $H\alpha$  flare emission at A2 and A3 at 15:23:00 UT as well as *Yohkoh*/HXR emission at about 15:23:30 UT were related to this impulsive reconnection. We further suggest that, as the result of the initial reconnection, a flux rope was formed, which immediately became unstable and erupted.

Further evolution of the erupting magnetic configuration is, however, less clear and more speculative. In Figure 7, we present two possibilities which differ by the structure of the large-scale magnetic field overlaying the active region.



*Figure 7.* April 9, 2001 flare and the CME were triggered by a tether-cutting type of reconnection in the core fields (red lines) which connected the innermost parts of the  $\delta$ -spot. A flux rope was formed (panels c and f, red lines), which immediately became unstable and erupted. Two possible developments of the April 9, 2001 flare are shown in the upper and lower panels. Upper panels: If coronal streamers existed above the active region (black lines in panels a–c), then the flare and the CME would evolve according to the “standard” flare model where the flare ribbons and the post-flare loops are formed due to main reconnection below the erupting field (panel c, blue lines). Lower panels: If the entire magnetic flux of the active region was enclosed by a large-scale overlying flux (black lines in panels d–f), then the erupting flux rope will break out from the enclosure by reconnecting with the overlying flux. Part of the flux will be transferred to the side lobe fields (green lines), while the rest will be pushed up in the corona, stretched and reconnected beneath the flux rope during the main reconnection process. We further suggest that after the main reconnection is exhausted and all core flux is cut off, these expanded lobe fields could eventually be dragged in the vertical current sheet and reconnected at the main reconnection site.

The butterfly-shaped image of the active region as seen in the 15:09 UT *Yohkoh* frame (Figure 4, left) seem to suggest that the  $\delta$ -spot was associated with two cusp-like structures (Figure 7a–c, black lines), which indicate the presence of coronal streamers above the active region. In this case, the flare and CME would evolve according to the “standard” flare model (McKenzie, 2002) and the post-flare loops will be formed due to the main reconnection below the erupting field (Figure 7c, blue lines). However, in this configuration, there are no direct magnetic connections between the reconnection site and the outer areas where the RBs appeared. Therefore, it is hard to explain the occurrence of these RBs. The only possibility is that a second reconnection may occur in the upper (cusp) region when the rising flux rope pushes through, but this reconnection is not very likely to occur so early in the main phase.

Another possibility is that the entire magnetic flux of this active region was enclosed by a large-scale overlying flux (black line in panels d–f of Figure 7). In this scenario, the erupting flux rope (red lines) will break out through the enclosure

by reconnecting with the overlying flux. Part of the “blue” flux will be transferred to the side lobe fields (Figure 7, green lines), while the rest of it will be pushed up in the corona, stretched and reconnected beneath the flux rope during the main reconnection process. This scenario is similar to the idea of external and internal reconnections presented in Figure 9 of Sterling and Moore (2004). Thus, slow type III RS bursts observed in this flare could be generated by the break-out type of reconnection (Antiochos, 1998; McNeice *et al.*, 2004) that supposedly occurred high in the corona and produced electron beams that directly propagate along the long trajectories downwards toward the photosphere. Those types of radio bursts are expected in the case of quadrupole reconnection configurations (Aschwanden, 2002), while bipolar and tripolar configurations are less suitable for their generation (mainly type III burst are expected). This scenario is also supported by the fact that the RBs appeared early in the event before A2 and A3 reached their maximum and soft X-ray flux was still very low. This implies that the second reconnection, the break-out type reconnection, occurred when the event was still at the beginning of the impulsive phase.

Regardless of the realized scenario (*i.e.*, “standard” model or break-out reconnection), post-flare loops and flare ribbons will be formed below the escaping flux rope due to main reconnection which could generate fast type III and type RS radio bursts that have been observed after 15:24 UT.

The post-flare loop system usually displays an apparent growth as the reconnection site above it moves upward with the velocity of order of tens of kilometer per second, as estimated from the flare ribbon separation (Qiu *et al.*, 2002; Wang *et al.*, 2004). We thus speculate that the slowly drifting radio structure with a mean velocity of about  $12 \text{ km s}^{-1}$  was probably associated with the termination shock above the growing post-flare loops. As the reconnection site moved upward, an extended current sheet may have formed below the plasmoid (Kliem, Karlický, and Benz, 2000) and become unstable, thus, generating secondary plasmoids (Shibata and Tanuma, 2001; Tanuma *et al.*, 2001). These plasmoids, or current-carrying loops, could interact through coalescence processes generating quasi-periodic main bursts as well as pulsations with shorter time scales as observed in this flare (see Tajima *et al.*, 1987; Karlický, 2004). Another possibility, although also complementary to the one discussed earlier, is that many individual magnetic fluxes could be interacting during this flare step-by-step at progressively higher heights in the corona such that electron beams, accelerated in these reconnections, bombard more and more distant remote sites, creating  $H\alpha$  brightenings.

As evidenced from Figures 2 and 4, the  $\delta$ -spot was also associated with two independent magnetic fluxes, or lobe fields, that connected A2–A1 and A3–A5 (Figure 7, green lines). As we mentioned earlier, some additional flux could be transferred to the side lobe fields via break-out type of reconnection, which will lead to the expansion of the lobe fields. We further suggest that after the main reconnection is exhausted and all core flux is cut off, these expanded lobe fields were eventually dragged in the vertical current sheet and reconnected at the main

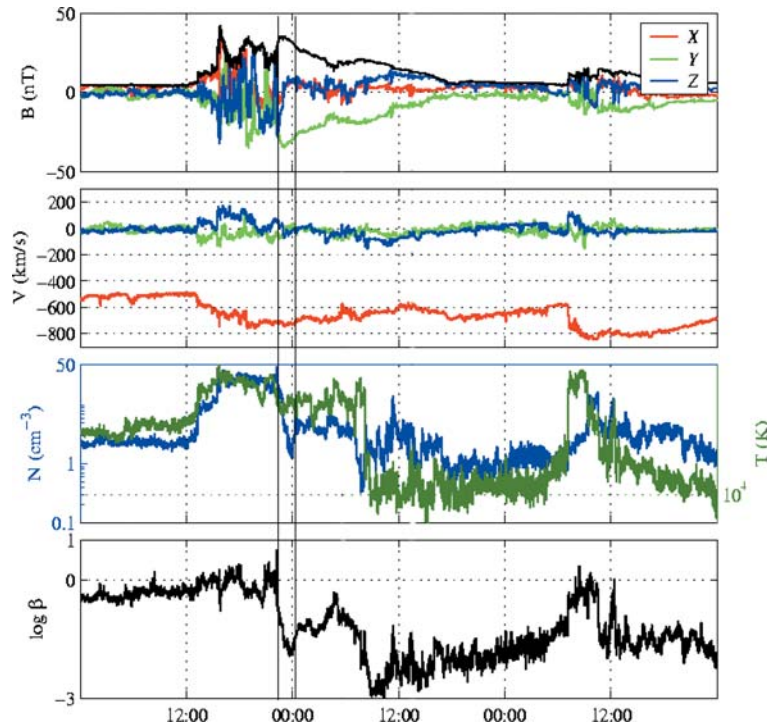


Figure 8. ACE data for the magnetic disturbance observed between April 11 and 13, 2001. The  $x$ -axis starts at midnight on April 11, 2001. Two vertical solid lines mark the boundary of a MC-like structure that was right handed with the axial field pointing westward and the azimuthal field direction changing from south to north.

reconnection site (Figure 7f). These lobe fields were clearly present in the active region before the flare, while they were seen to be less intense and more diffuse in the after flare image (see 15:09 UT *Yohkoh* image in Figure 4). The increase in the gyro-synchrotron emission at 15:28 UT starts nearly at the same time as the RB at the footpoint of the lobe fields in Area 1 (Figures 1 and 3) supports this suggestion. It is not clear, however, whether or not the new field lines that were formed by the lobe field reconnection further erupted and followed the escaping core fields.

In Figure 8, we plot Advanced Composition Explorer (ACE) measurements obtained between April 11 and 13, 2001. The data show that between 15:00 UT on April 11 and 16:00 UT on April 12 a strong extended magnetic disturbance was observed in the solar wind. Zhao (2001) concluded that this disturbance was associated with two halo CMEs that erupted from AR NOAA 9415 on April 9 at 15:54 UT (event in this study) and on April 10 at 05:26 UT. The April 10 CME was much faster than the April 9 CME, and the cone model confirmed that the faster CME was able to catch up with the slower one (Zhao, 2001). The shock, associated with the April 9 and 10 eruptions, is seen between 13:00 and 22:30 UT

on April 11, while the magnetic structures observed after 05:30 UT on April 12 were associated with the eruption on April 10. We then speculate that the magnetic structure, observed between 22:30 UT on April 11 and 05:30 UT on April 12, could be related to the April 9 eruption. A magnetic cloud (MC) like structure, which follows the shock, is indicated in Figure 8 by the two vertical lines. It is interesting to note that a strong westwardly directed negative  $B_y$  component of the interplanetary magnetic field (top graph, lower line) is persistently present in the disturbance, while the  $B_z$  component was weak and rotating. It gradually changed its sign from negative (southward directed) to positive (northward directed). Thus, negative  $B_y$  and rotating  $B_z$  components are indicative of a right-handed MC, where the azimuthal magnetic field changes its direction from south to north, while the axial field points westward.

The orientation of this cloud as well as the presence of strong westward component does not agree with the orientation of the erupted core field, if we assume that the interplanetary CME preserves its initial orientation. One explanation is that the reconnected lobe fields could also become part of the CME. The positively twisted magnetic loop connecting A1 and A5 had a strong westwardly directed axial field, while the polarity of its leading edge was negative. In this case, the lobe fields could be responsible for the strong negative  $B_y$  component that followed the MC-like structure.

Finally, we would like to point out that the ACE data seems to suggest that the magnetic structure between 22:30 UT on April 11 and 18:00 UT on April 12 was not monolithic but rather consisted of many small-scale features that could be classified as MCs or MC-like structures. If so, it then implies that several individual plasmoids were formed during the eruption, which was suggested earlier based on the analysis of the radio data.

In summary, we conclude the following. The timing of the event, *i.e.*, the fact that the initial brightenings (A2 and A3) associated with the core flux began earlier than the RB argues against the break-out reconnection in the early phase of the eruption. We thus conclude that the M7.9 flare and the CME were triggered by a tether-cutting reconnection deep in the core field of the  $\delta$ -spot. Further evolution of the erupted flux rope could proceed either according to the “standard” or a break-out model. No solid conclusion can be made as to which scenario was realized in the event. Nevertheless, the complex structure of the flare, the emission in visible, X-ray, and radio spectral ranges point toward a scenario which involves multiple reconnection processes between extended closed magnetic structures.

### Acknowledgement

We thank referee Bernhard Kliem for valuable suggestions and constructive criticism which improved the clarity of the paper. We are obliged to the BBSO staff for their effort in obtaining the data and to A. Klassen for making the Potsdam

radio spectrum available to us. We thank the ACE MAG instrument team and the ACE Science Center for providing the ACE data. SOHO is a project of international cooperation between ESA and NASA. VY work was supported under NSF grant ATM 0205157 and NASA NNGO 4GJ51G. MK acknowledges support under grant A3003202 of Academy of Sciences, Czech Republic. Qiang Hu's work was supported by NASA grant NNG04GF47G.

## References

- Antiochos, S.K.: 1998, *Astrophys. J.* **502**, L181.
- Asai, A., Ishii, T.T., Kurokawa, H., Yokoyama, T., and Shimojo, M.: 2003, *Astrophys. J.* **586**, 624.
- Aschwanden, M.J.: 2002, *Space Sci. Res.* **101**, 188.
- Cecatto, J.R., Sawant, H.S., Fernandes, F.C.R., Krishan, V., Rosa, R.R., and Karlický, M.: 2002, in P.C.H. Martens, D. Cauffman (eds.), *Multi-Wavelength Observations of Coronal Structure and Dynamics*, Proceedings of the *Yohkoh* 10th Anniversary Meeting, COSPAR Coll. Ser. **313**.
- Harra, L.K., Matthews, S.A., and van Driel-Gesztelyi, L.: 2003, *Astrophys. J.* **598**, L59.
- Hurford, G.J., Schwartz, R. A., Krucker, S., Lin, R.P., and Smith, D.M.: 2003, *Astrophys. J.* **595**, L77.
- Karlický, M.: 2004, *Astron. Astrophys.* **417**, 325.
- Kliem, B., Karlický, M., and Benz, A.O.: 2000, *Astron. Astrophys.* **360**, 715.
- LaBonte, B.: 1976, *Solar Phys.* **50**, 201.
- Liu, C., Deng, N., Liu, Y., Falconer, D., Goode, P.R., Denker, C., and Wang, H.: 2005, *Astrophys. J.* **622**, 722.
- MacNeice, P., Antiochos, S.K., Phillips, A., Spicer, D.S., DeVore, C.R., and Olson, K.: 2004, *Astrophys. J.* **614**, 1028.
- Manoharan, P.K., van Driel-Gesztelyi, L., Pick, M., and Démoulin, P.: 1996, *Astrophys. J.* **468**, L73.
- McKenzie, D.E.: 2002, in P.C.H. Martens and D. Cauffman (eds.), *Multi-Wavelength Observations of Coronal Structure and Dynamics*, Proceedings of the *Yohkoh* 10th Anniversary Meeting, COSPAR Coll. Ser. **155**.
- Moore, R.L. and LaBonte, B.: 1980, in M. Dryer, E. Tandberg-Hanssen (eds.), *Solar and Interplanetary Dynamics*, Reidel, Boston, *IAU Symp.* **91**, 207.
- Moore, R.L., Sterling, A.C., Hudson, H.S., and Lemen, J.R.: 2001, *Astrophys. J.* **552**, 833.
- Pevtsov, A.A.: 2000, *Astrophys. J.* **531**, 553.
- Qiu, J., Lee, J., Gary, D.E., and Wang, H.: 2002, *Astrophys. J.* **565**, 1335.
- Sakurai, T. and Hagino, M.: 2003, *Adv. Space Res.* **32**, 1943.
- Shibata, K. and Tanuma, S.: 2001, *Earth Planet Space* **53**, 473.
- Sterling, A.C. and Moore, R.L.: 2004, *Astrophys. J.* **613**, 1221.
- Tajima, T., Sakai, J.I., Nakajima, H., Kosugi, T., Brunel, F., and Kundu, M.R.: 1987, *Astrophys. J.* **321**, 1031.
- Tang, F. and Moore, R.L.: 1982, *Solar Phys.* **77**, 263.
- Tanuma, S., Yokoyama, T., Kudoh, T., and Shibata, K.: 2001, *Astrophys. J.* **551**, 312.
- Tarnstrom, G.L. and Zehntner, Ch.: 1975, *Nature* **258**, 693.
- Thompson, B.J., Plunkett, S.P., Gurman, J.B., Newmark, J.S., St. Cyr, O.C., and Michels, D.J.: 1998, *Geophys. Res. Lett.* **25**, 2465.
- Tian, L., Liu, Y., and Wang, J.: 2002, *Solar Phys.* **209**, 361.
- Wang, H.: 2005, *Astrophys. J.* **618**, 1012.
- Wang, H., Chae, J., Yurchyshyn, V., Yang, G., Steinegger, M., and Goode, P.R.: 2001, *Astrophys. J.* **559**, 1171.

- Wang, H., Gallagher, P., Yurchyshyn, V., Yang, G., and Goode, P.: 2002, *Astrophys. J.* **569**, 1026.
- Wang, H., Goode, P., Denker, C., Yang, G., Yurchyshyn, V., Nitta, N., Gurman, J.B., and St. Cyr, O.C.: 2000, *Astrophys. J.* **536**, 971.
- Wang, H., Qiu, J., Jing, J., Spirock, T.J., Yurchyshyn, V., Abramenko, V., Ji, H.S., and Goode, P.R.: 2004, *Astrophys. J.* **605**, 931.
- Yurchyshyn, V., Wang, H., Abramenko, V., Spirock, T.J., and Krucker, S.: 2004, *Astrophys. J.* **605**, 546.
- Zhao, X.P.: 2001, *AGU Fall Meeting*, No. SH12A-0736.